New Journal of Physics
The open-access journal for physics

Monte Carlo simulation of non-conservative positron transport in pure argon

M Šuvakov[1], Z Lj Petrović[1,4], J P Marler[2], S J Buckman[3], R E Robson[3] and G Malović[1]

[1] Institute of Physics, University of Belgrade, PO Box 68, 11080 Zemun Serbia
[2] University of Aarhus, Aarhus, Denmark
[3] Centre for Antimatter-Matter Studies, Research School of Physical Sciences and Engineering, Australian National University, Canberra, ACT, 0200 Australia
E-mail: zoran@phy.bg.ac.yu

New Journal of Physics **10** (2008) 053034 (19pp)
Received 11 March 2008
Published 28 May 2008
Online at http://www.njp.org/
doi:10.1088/1367-2630/10/5/053034

Abstract. The main aim of this paper is to apply modern phenomenology and accurate Monte Carlo simulation techniques to obtain the same level of understanding of positron transport as has been achieved for electrons. To this end, a reasonably complete set of cross sections for low energy positron scattering in argon has been used to calculate transport coefficients of low energy positrons in pure argon gas subject to an electrostatic field. We have analyzed the main features of these coefficients and have compared the calculated values with those for electrons in the same gas. The particular focus is on the influence of the non-conservative nature of positronium formation. This effect is substantial, generally speaking much larger than any comparable effects in electron transport due to attachment and/or ionization. As a result several new phenomena have been observed, such as negative differential conductivity (NDC) in the *bulk* drift velocity, but with no indication of any NDC for the *flux* drift velocity. In addition, there is a drastic effect on the bulk longitudinal diffusion coefficient for positrons, which is reduced to almost zero, in contrast to the other components of the diffusion tensor, which have normal values. It is found that the best way of explaining these kinetic phenomena is by sampling real space distributions which reveal drastic modification of the usual Gaussian profile due to pronounced spatial differentiation of the positrons by energy.

[4] Author to whom any correspondence should be addressed.

Contents

1. Introduction

Positron interactions with atoms and molecules [1] are fundamentally different from those of electrons. For example, in the case of positrons the exchange interaction is not possible. Additionally, for positrons, positronium (an 'atom' consisting of a positron and an electron) formation is possible (as either an open or closed, 'virtual', channel). Recent advances in experimental measurements of high resolution, low energy, inelastic positron impact scattering confirm that there are significant differences between electron and positron cross sections [2, 3]. Additionally, benchmark measurements for noble gas atoms, confirmed by two independent measurements, show that the positronium (Ps) formation cross section is quite large for these atoms [4, 5]. An area which remains to be tested is transport measurements for positrons. Considering the significant difference between the cross sections, it was expected that the transport coefficients would also be significantly different. This is especially the case given the presence of the non-conservative (with respect to particle number) nature of Ps formation. Therefore, one might expect that positron transport in rare gases might be the ideal place to test the regime of hypothesized negative differential conductivity (NDC) [6] as a result of non-conservative collisions.

In addition to highlighting interesting fundamental physics, transport coefficients can be used for modeling thermal positrons in gaseous and liquid environments. As thermal distributions are, in general, the situation for most practical applications of positrons, understanding positron transport may be crucial to improving positron diagnostics in medicine [7] and biology, or other material science applications (e.g. [8, 9]). While considerable effort has been invested in modeling of thermalization of positrons starting from high energies [10]–[12] very little has been done on thermalization of positrons at energies close to and below the excitation energy thresholds [13]. With the development of the Penning–Malmberg–Surko trap [14] as a primary tool for numerous experiments and possible applications (e.g. [15]) modeling of positron thermalization below 20 eV becomes at least interesting, if not crucial, in further optimizations of the trap. As the conditions in such traps are halfway between collision-free and swarms in hydrodynamic equilibrium, application of techniques developed for non-hydrodynamic transport [16, 17] is also of interest.

Applying standard techniques developed for electrons to the positron situation has been limited. One example is the discussion of positron swarms in a paper by Robson [18] where the focus was on non-conservative processes and their effect on transport properties [19]–[21]. In [18], general expressions for non-conservative correction terms which were *independent* of the loss mechanism were derived. These expressions were applied to ion–molecule reactions, electron attachment and positron annihilation. That analysis carries over directly to the positron swarms discussed here, where Ps formation is the dominant mechanism, and the non-conservative corrections to transport properties may be estimated accordingly as to complement the Monte Carlo results.

In this paper, we have performed calculations of swarm parameters: drift velocity, components of the diffusion tensor, mean energies, characteristic energies and rate coefficients. We will also show special calculations of spatial profiles of swarm density and different parameters such as rates. Calculations were made for the range of E/N covering mean energies up to 10 eV. The most striking effect that was found, and will be discussed later, was the occurrence of NDC for only one type of drift velocity (the one that should be used in the diffusion equation to model realistic experiments—the bulk drift velocity) while no NDC exists for the other type of drift velocity (the one that is to be used in flux calculations—the flux drift velocity). In the case of electrons, NDC was always found to exist in both the types of drift velocities and also it was essential that conditions for NDC were first met in the flux drift velocity.

For the purpose of this paper, NDC will be defined as the decrease of the drift velocity with an increase of the normalized electric field E/N. In principle, one could multiply the drift velocity by the number density to get the conductivity but the dependence of the drift velocity itself is of fundamental interest, and thus we focus on NDC as defined with the focus on drift velocity [22]. NDC is found to occur when momentum and energy controlling rates have different E/N dependences which also favor the NDC (a rapid increase of the rate of momentum transfer collisions in parallel to a decay of the rate of inelastic collisions). The origin of NDC has been explained by a number of authors, and basically depends on the shapes of the elastic and inelastic cross sections, see section 4.3 [6], [22]–[24]. Note that although the mean velocity decreases when E/N is increased, the mean energy and the mean absolute value of the velocity $\langle|\mathbf{v_i}|\rangle$ increase.

NDC for electrons was found to occur also in mixtures of rare gases (especially with helium) at E/N below the threshold for inelastic processes, when elastic scattering on helium begins to control the energy balance, whereas the momentum balance is dominated by the elastic scattering for the other rare gas. However, it may not be expected in a pure atomic gas at E/N too low for inelastic processes.

Studies focusing on electrons can also give insight into the positron situation. One example is the paper of Vrhovac and Petrović [6], which gives a theory of NDC stressing how non-conservative processes could affect and even induce the NDC. While this paper was focused on effects in electrons, this study is highly relevant for positrons given that, in most systems, positrons have a significant non-conservative cross section (i.e. Ps formation—the formation of positronium inevitably leads to annihilation and loss of the positron altogether).

Additionally, it is worth noting that recently a number of kinetic phenomena in electron interactions have been identified and explained [25]–[28] and that most of those were associated with some form of non-conservative transport. Thus, it could be expected that these phenomena may be observed in positron transport as well. Finally, we note that there have been attempts to measure drift velocities [29, 30] and annihilation rates [11, 31] of positrons in gases.

This paper looks at the main features of positron transport, focusing on the phenomena that can be seen in the transport of particles which experience very pronounced non-conservative collisions. A complete set of cross sections for a particular gas is required for modeling of transport processes. By complete we mean that such sets should provide total energy and momentum balance [32]. These are now available due to recent advances in experimental techniques which have enabled measurements of a wide range of inelastic cross sections for positron scattering on atoms and molecules and a renewed interest in theoretical studies for positron scattering at low energies [33]. At this point we are, however, still limited by the accuracy of the experimental data available. New experiments which would improve the normalization of the cross sections and/or provide accurate experimental transport data will be important to improving our simulations. In the meantime, these results provide the first steps for modeling of applications involving positrons on the basis of the currently available theory, simulation techniques and experimental cross-section data.

2. Cross section set for positron scattering from argon

The cross section set for positron interactions with argon has been based on a variety of measurements and calculations which are available in the literature. The cross section set used in this paper is shown in figure 1. In our set, we use the elastic momentum-transfer cross section (MTCS) and assume isotropic scattering. The Monte Carlo code may use the total cross section, but in that case differential scattering would have to be added for different energy regions complicating the final set. The choice of the MTCS must, however, be based on data in the literature for the total cross section, as there is little data available for the MTCS, and certainly no experimental determinations. On the other hand, there have been a number of absolute determinations of the total cross section as a function of energy. The most recent of these measurements is the work of Karwasz *et al* [34], who also provide a comprehensive summary of the earlier work and the level of the agreement between experiment and theory. This comparison indicates some large disparities (50%) within and between both experiment and theory. Given that we required the energy dependence of the elastic MTCS, an ideal solution was to choose a theoretical approach for which this was readily available. Elastic MTCS have recently been calculated by McEachran [35] in an update of their earlier calculation shown in Karwasz *et al* [35]. For the total cross section this calculation is in reasonable agreement with the experimental values of Karwasz *et al* [35] and shows a similar energy dependence to other theoretical work (e.g. Gianturco *et al* [36]). As the values of the MTCS from this calculation were readily available on a fine energy grid, including down to zero energy, we have chosen to use it as the basis for our elastic MICS. It is also important to note that we had decided to use a different set of data for elastic momentum transfer the values of the transport coefficients would definitely change, but the kinetic effects discussed here would still be the same with identical explanations.

Experimental results have recently become available for the electronic excitation of the two lowest lying $3p_5 4s$ $J = 1$ levels of argon [37]. Note that these are the only two levels of the 4s manifold that are accessible by positron excitation. Calculations of these excitation cross sections have also been carried out by Parcell *et al* [38] and these two determinations have been used to construct an effective cross section for these excited states. We have also added in a cross section for positron impact excitation of higher singlet levels based on that for electron impact excitation of argon [39].

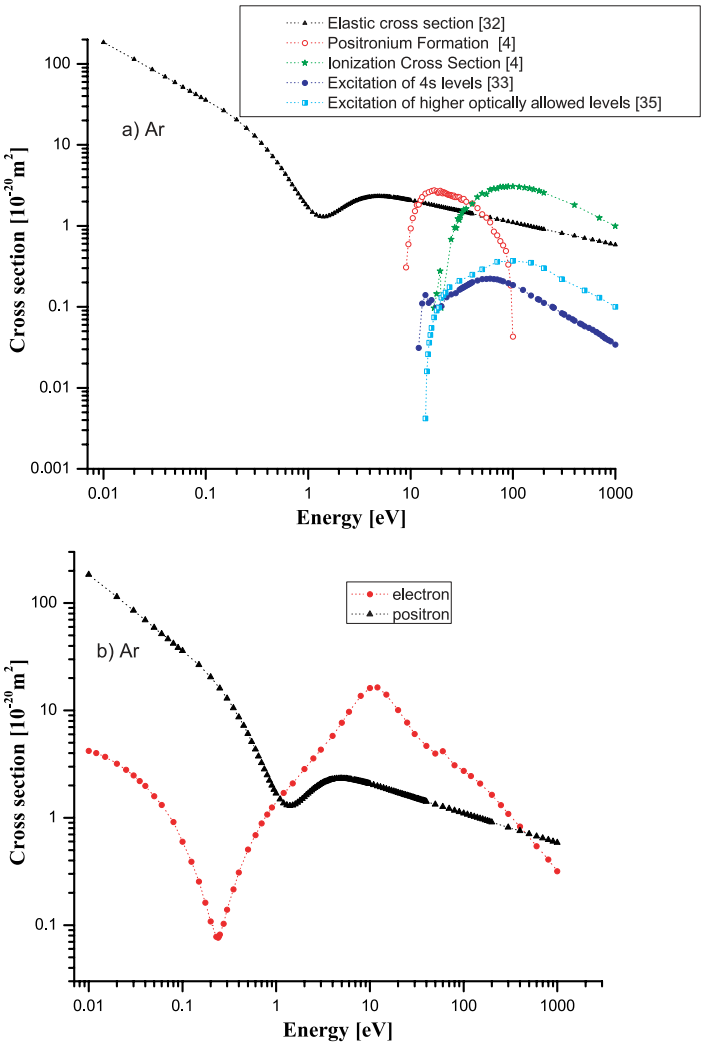

Figure 1. (a) Complete cross section set for positrons in argon. References to the sources are given in the text. (b) Comparison between elastic MTCS for electrons and positrons in argon.

The Ps formation and ionization cross sections were taken from the work of Marler *et al* [4]. These resulted from a technique which directly measures the Ps cross section and they are in good quantitative agreement with an alternative approach by Laricchia *et al* [5]. Direct annihilation has been neglected. This is reasonable for the noble gas systems as the direct annihilation cross section is known to be several orders of magnitude lower than that for Ps formation [40].

As the energy dependence of both the elastic and inelastic cross sections for electrons and positrons is completely different, we may expect aspects of positron transport to differ significantly from those of electrons. Yet, there is no reason why basic features and absolute values should be outside the same order of magnitude for all coefficients. Ps formation will lead to the loss of positrons, and therefore will be analogous to electron attachment in electron transport. However, in this case, ionization will not lead to an increase of the number of positrons so it should be treated as an inelastic, conservative process.

3. Monte Carlo code

We have performed calculations by using a new Monte Carlo program that has been tested to give good benchmark results for electrons, especially in the treatment of non-conservative transport [41]–[43]. The code is based on a time integration technique (as opposed to the more standard null-collision technique) which is more appropriate for spatially and temporally variable fields. The code is designed to include thermal effects, superelastic and all kinds of standard collisions, as well as the effect of magnetic fields. For electrons, we have found that typical agreement and reproducibility, provided that a sufficient number of electrons are involved, is better than 0.1% given sufficient computation time.

The code first follows charged particles from the initial conditions until hydrodynamic quasi-steady state conditions are achieved. The code also describes thermalization from whatever was selected as the initial set of conditions. This stage is the most time consuming. In order to reduce this computation time, the charged particles that have reached equilibrium with the field are sampled repeatedly at times uncorrelated with the times of collisions. Typically, we followed 100000 positrons through a large number of collisions. All simulations were performed at a gas number density corresponding to a pressure of 1 Torr. Standard measures to speed up the code and to compensate for non-conservative processes have been implemented.

In Monte Carlo simulations, the bulk (B) transport coefficients may be determined from the rate of change of the appropriate averages of the positions of the swarm particles in *configuration* space. The number-changing reaction rate is defined by

$$\omega^{(0)} = -\frac{\mathrm{d}}{\mathrm{d}t}\ln(N), \tag{1}$$

the drift velocity by

$$\boldsymbol{\omega}^{(1)} = \mathbf{W}_{\mathrm{B}} = \frac{\mathrm{d}}{\mathrm{d}t}\langle \mathbf{r} \rangle , \tag{2}$$

and the diffusion tensor by

$$\boldsymbol{\omega}^{(2)} = \mathbf{D}_{\mathrm{B}} = \frac{1}{2}\frac{\mathrm{d}}{\mathrm{d}t}\langle \mathbf{r}^{*}\mathbf{r}^{*} \rangle , \tag{3}$$

where N is the total number of charged particles at any moment and $\mathbf{r}^{*} = \mathbf{r} - \langle \mathbf{r} \rangle$. The flux (F) drift velocity components and the flux diagonal elements of the diffusion tensor are given by

$$\mathcal{W}_{\mathrm{F}i} = \frac{\mathrm{d}\mathbf{r}_i}{\mathrm{d}t} = \langle \mathbf{v_i} \rangle, \tag{4}$$

$$\mathcal{D}_{\mathrm{F}ii} = \langle r_i v_i \rangle - \langle r_i \rangle \langle v_i \rangle , \tag{5}$$

where v_i is the instantaneous velocity of individual charged particles, averaging is performed over all particles and $i = x$, y and z.

4. Transport of positrons in argon

We have calculated transport coefficients for positrons in pure argon in the region where the Ps formation is significant. The results are shown below and compared to those for electrons where possible. As we proceed through this section it is helpful to recall the general observation, valid for all types of charged particles, that a loss mechanism governed by a rate which *increases* with

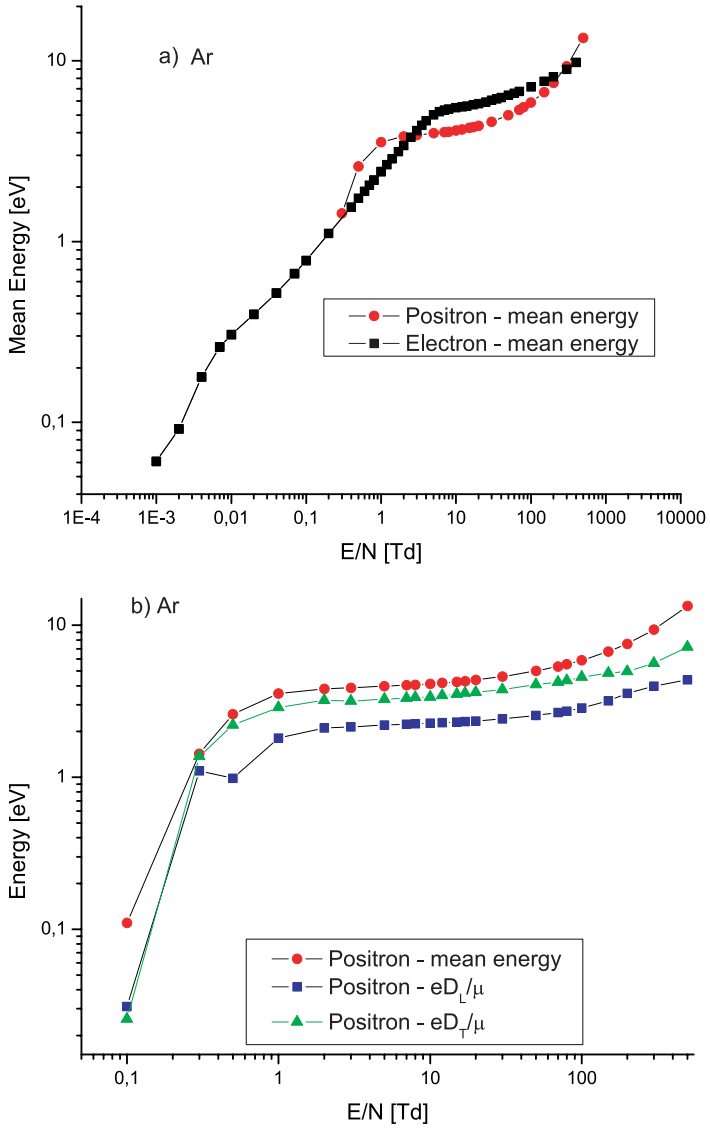

Figure 2. The mean energy (a) for positrons and electrons and characteristic energies (b) for positrons in pure argon as a function of the reduced electric field E/N. The data for electrons were obtained from one of the standard sets of cross sections [48].

energy leads to an overall cooling of the swarm, i.e. to a lowering of the mean energy, and a reduction in the measured (bulk) drift [18], [44]–[47].

Based on an inspection of cross sections alone, one would anticipate some differences between transport coefficients for electrons and positrons, but nevertheless, the two sets of drift velocities were expected to be of a similar order of magnitude.

In figure 2(a) we show the mean energy for both electrons and positrons. The E/N dependencies of the mean energies are quite different for each but the two quantities are relatively close in magnitude. In general, one would expect the mean energy of positrons to be higher at the same E/N (the unit for E/N is Townsend: $1\,\mathrm{Td} = 10^{-21}\,\mathrm{V\,m^2}$), due to a smaller number of available inelastic channels. However, the Ps formation rate increases with energy

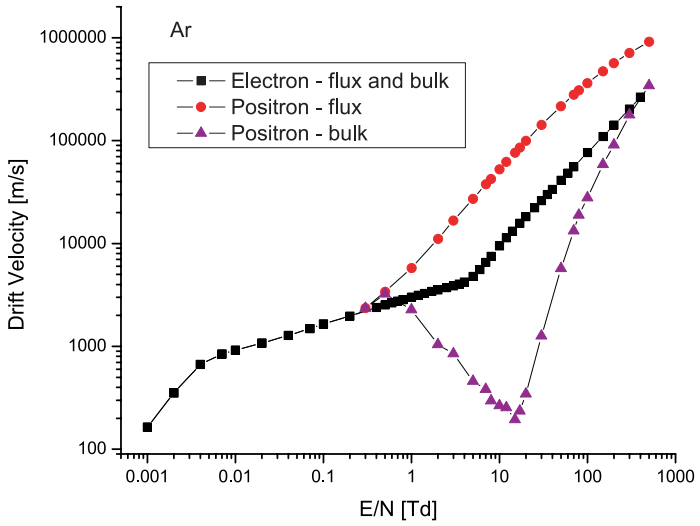

Figure 3. Drift velocities of electrons and positrons in pure argon.

in this range, and therefore this process effectively cools the energy distribution function by selectively removing the higher energy positrons. This leads to a lower mean energy of positrons in the E/N range where Ps formation is dominant. In figure 2(b) we compare the positron mean energy with the characteristic energies defined as the ratios eD_T/μ and eD_L/μ, (here $\mu = enw$ is the mobility, D_L and D_T are longitudinal and transverse components of the diffusion tensor, while both diffusion and mobility are the flux coefficients) for positrons in argon. Mean energy and characteristic energy (eD_T/μ) are similar in magnitude and have a similar E/N dependence, while eD_L/μ has a similar magnitude to the other two but departs from eD_T/μ at E/N values above 0.2 Td. Still the difference is not more than a factor of 2.5.

4.1. Drift velocities and NDC

In figure 3, we compare the flux and bulk drift velocities for positrons and electrons. The flux drift velocity is what is determined via the flux-gradient equation, i.e. Fick's law, but it is not in general measurable. The measurable drift velocity is referred to as the bulk drift velocity and is the quantity which appears in the diffusion equation [46, 49, 50]. The diffusion equation therefore provides the relationship between what is measurable and the desired transport coefficients. The same remarks apply to the flux and bulk diffusion coefficients. The bulk quantities take into account, both explicitly and implicitly, the loss or gain of particles to the system. When non-conservative effects are negligible, the two sets of transport properties coincide. Thus, for electrons in rare gases such as argon, the flux and bulk drift velocities are effectively the same at low E/N. Small but significant differences arise as E/N is increased, i.e. where ionization (the only non-conservative processes available in that system) becomes significant. As shown in figure 3, the electron and positron flux drift velocities have a qualitatively similar dependence upon E/N and any difference in magnitude can be largely explained by the difference in magnitudes of scattering cross sections for the two types of particles. For electrons, the bulk and flux drift velocities in argon are effectively the same in this range of E/N, as explained above. On the other hand, for positrons, the flux and bulk drift velocities are markedly different, both qualitatively and quantitatively, due to the effect of non-conservative Ps formation, which has no counterpart for electrons in argon.

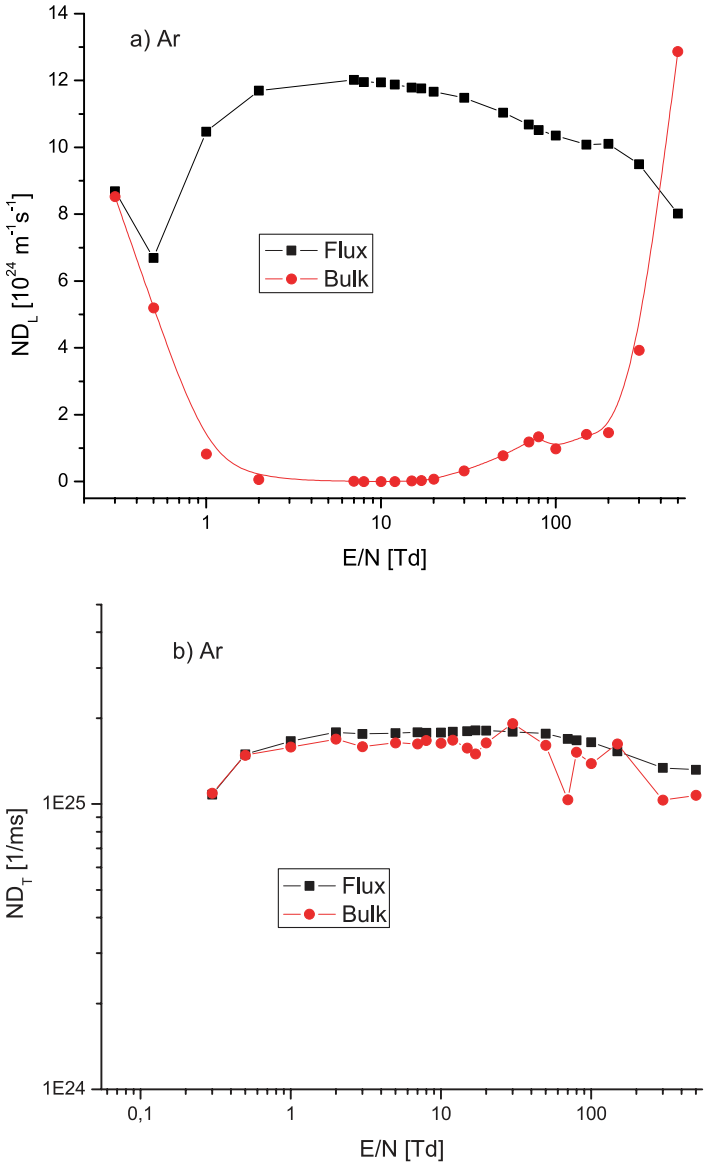

Figure 4. The components of the (a) longitudinal and (b) transverse diffusion tensor as a function of the reduced electric field E/N. The bulk properties have a larger fluctuation of points due to the differentiation required to calculate them.

Figure 3 shows the difference between the flux and bulk drift velocities for positrons is as large as several orders of magnitude. Specifically, the bulk drift velocity becomes very small and reaches a minimum around 15 Td. The magnitude of the positron flux drift velocity maintains expected values and increases monotonically with E/N. In contrast, the bulk drift velocity decreases with increasing E/N in the range 1–15 Td, i.e. it displays the NDC effect [6, 22, 23].

4.2. Diffusion and rate coefficients

Longitudinal and transverse components of the diffusion tensor are shown in figure 4. While transverse diffusion behaves in an expected manner, i.e. similar to electrons (figure 4(b)),

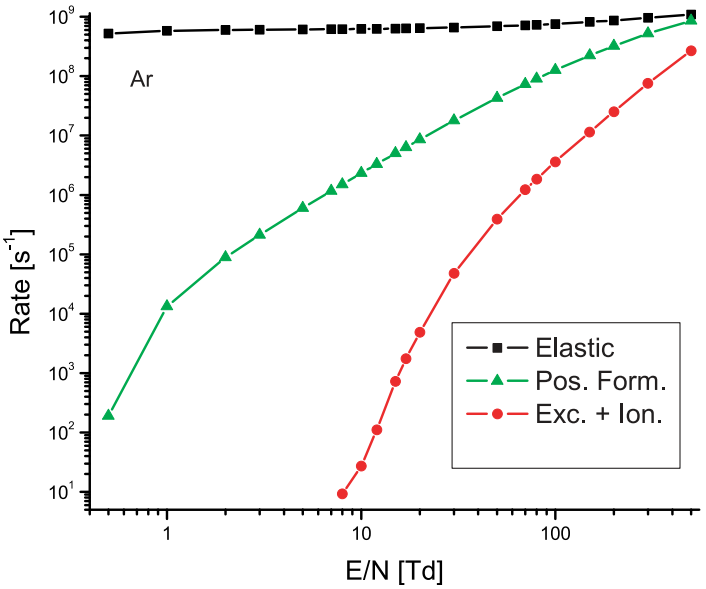

Figure 5. Rate coefficients of elastic, Ps formation and inelastic collisions of positrons in argon.

with only a small difference between the values for the flux and the bulk coefficients, the bulk longitudinal diffusion coefficient shows a deep minimum with respect to E/N. Over a broad range of E/N, the longitudinal bulk diffusion coefficient is more than two orders of magnitude below the flux diffusion coefficient. That is, the positrons in an experiment would appear to diffuse very slowly along the direction of the electric field. Interestingly, a minimum in longitudinal diffusion is also the signature of inelastic collision-induced NDC [23], discussed further below.

Figure 5 shows rate coefficients for elastic collisions, Ps formation and all other inelastic processes. While the elastic collision rate is very slowly varying, the Ps formation rate increases steeply and attains high values at even moderately high E/N, well below the onset of the growth of the rate for other inelastic processes. Therefore, Ps formation dominates the region where all the observed NDC effects occur. This provides indirect evidence that the NDC effect reported here is entirely due to non-conservative Ps formation and not to other inelastic processes as will be further demonstrated below.

As an aside, this sheds light on why argon is not a good choice as a cooling gas for positron traps. Due to the large Ps formation cross section at energies below the threshold for electronic excitation, losses at these low energies are high, and thermalization is inefficient. A good thermalizing gas would have both low excitation thresholds and a significant rate of inelastic collisions competing with the rate of Ps formation, thereby allowing positrons the chance to lose their energy and drop below the threshold for Ps formation.

4.3. Explanation of NDC induced by a non-conservative process (Ps formation)

Firstly let us recall the physical origin of the difference between the flux and bulk drift velocities. If one has, for example, a pulse of positrons traveling in the direction of the applied electrostatic field, those particles at the leading edge have a somewhat higher energy than those at the rear, and hence, since the loss through Ps formation increases with increasing energy (at least in

the range of fields considered here), positrons are lost preferentially at the front of the pulse. This effectively reduces the velocity of the center-of-mass of the positron pulse—ensemble (see equation (2)), i.e. the bulk drift velocity $\mathbf{W_B}$. This retardation is represented mathematically by a correction term to the average or flux drift velocity $\mathcal{W}_\mathrm{F}$ of equation (4), either exactly as in equation (3b) of [51], or approximately and perhaps more usefully through the fluid (momentum transfer) theory [19]:

$$\mathbf{W_B} = \mathcal{W}_\mathrm{F} - \frac{2\epsilon}{3e}\frac{\mathrm{d}\alpha}{\mathrm{d}E}. \tag{6}$$

Here, α is the average Ps formation rate shown in figure 5 and ϵ is the mean positron energy.

Formally, the general condition for NDC is found by direct differentiation of equation (6) [6]:

$$\frac{\partial \mathbf{W_B}}{\partial E} = \frac{\partial \mathcal{W}_F}{\partial E} - \frac{2}{3e}\left[\frac{\partial \epsilon}{\partial E}\frac{\partial \alpha}{\partial E} + \frac{\epsilon \partial^2 \alpha}{\partial E^2}\right] \leqslant 0, \tag{7}$$

but it is found more useful to work with equation (6) directly, and substitute numerical values in the right-hand side.

Conditions for NDC in $\mathcal{W}_\mathrm{F}$ have been given by [6, 22, 23]. Since the Ps formation rate, α, and the field derivative $\partial\alpha/\partial E > 0$ (see figure 5), it is conceivable, as first pointed out by Vrhovac and Petrović [6], that the correction term in equation (6) may induce NDC in $\mathbf{W_B}$, even if $\mathcal{W}_\mathrm{F}$ is monotonically varying with field. Furthermore, if the correction term becomes comparable with $\mathcal{W}_\mathrm{F}$, then $\mathbf{W_B}$ may be small. Substitution of representative values from figures 2, 3 and 5 in the right-hand side of equation (6) indicates that both these possibilities are realized for positrons in argon in the range of E/N for which $\mathbf{W_B}$ exhibits NDC and dips to unusually low values (figure 3). The origin of these effects would, therefore, seem to be firmly attributable to the large, energy-selective Ps formation rate.

One question that immediately arises is whether it is possible that the second term on the right-hand side of equation (6) ever dominates the first term, making $\mathbf{W_B}$ negative. The analysis of Robson *et al* [45] indicates that the second-law of thermodynamics would preclude such a possibility. Thus, while $\mathbf{W_B}$ can decrease with E/N and even become very small, it cannot become negative. This is consistent with the results of our present calculations.

We now turn to electrons, where the relevant loss or gain mechanisms are attachment and ionization, respectively, and ask whether a similar phenomenon might occur there. It is useful to consider the example of [6], where it was shown that the second term in equation (6) may indeed lead to NDC in $\mathbf{W_B}$. However, for electrons, dissociative attachment cross sections are typically small, two orders of magnitude smaller than the MTCS, and ionization becomes very large only at high energies. It seems that one could not achieve the other conditions necessary for non-conservative collision-induced NDC, i.e. NDC could be seen in the bulk drift velocity only. Thus, [6] reaches the conclusion that, while their prediction for electrons is perhaps possible in principle, it probably cannot be realized. That is there would have to be either an NDC or a plateau in $\mathcal{W}_\mathrm{F}$ for NDC to also exist in $\mathbf{W_B}$. Neither would there be expected to be such a large difference (up to two orders of magnitude) at moderately high values of E/N between the bulk and flux values for electron swarms. The fact that such effects are observed for positrons is due to the large magnitude of the Ps formation cross section.

Finally, we note that even apart from NDC effects, positron swarms should provide an interesting system to hunt for other kinetic effects [21, 46] caused by non-conservative processes.

4.4. Further considerations of Ps formation

Returning to NDC we may conclude that for positrons in argon it occurs in the most unlikely place if one judges that by the conditions previously set out [6, 22, 23]. NDC is seen where, in principle, only elastic processes and Ps formation occur (see figure 5). Thus, the flux drift velocity, $\mathcal{W}_F$, rises with a relatively high slope, as there are no energy controlling processes there. So the bulk drift velocity NDC could only be the result of Ps formation in that range. If we use the data from figures 2 and 5 in equation (6) the predicted bulk drift velocity is considerably smaller than the flux and NDC is observed but the resulting bulk drift velocity is not exactly the same as calculated by our code. Nevertheless, it is easy to check with simulations that it is the Ps formation which causes the effect. If we turn off Ps formation there is no NDC, and the bulk and flux drift velocities are identical. However, if we instead consider an inelastic 'Ps formation' process, we have a chance of producing NDC but only if the system satisfies standard criteria as outlined in [6, 22, 23].

In all the cases, of course, when Ps formation occurs, very rapidly annihilation follows and positrons are lost. In this case, however, we have made model calculations by 'turning off' the non-conservative nature of the Ps formation, and we have assigned it to be an inelastic process. In figure 6(a) we show results for the drift velocities of positrons obtained assuming Ps formation acts as an inelastic process (i.e. with positron energy loss equal to the threshold for Ps formation). Bulk and flux drift velocities are as identical as different numerical procedures and statistical error of the Monte Carlo simulation will allow (one should pay attention that they are sampled by very different procedures). This is evidence that it is the non-conservative nature of the Ps formation that is causing the effect. We note again it is not just the changing numbers of positrons in the simulation (we have been comparing drift velocities here not the conductivity) and it is not in the shape of the Ps formation cross section but in the effect of the number changing nature of the process on the distribution functions. Figure 6(b) shows inclusion of Ps formation as an inelastic process also changes the mean energy albeit slightly; it becomes smaller for the same E/N.

A case like this could not be found for electrons (except in model calculations) where non-conservative processes (in this case attachment) could change the drift velocity from a plateau for the flux to the NDC for the bulk.

4.5. Spatial profiles of positron swarms

In considering charged particle transport it is often extremely useful to look at the energy distribution functions in order to make conclusions about the underlying physics of some processes. This is usually associated with the need to explain flux properties, and one such example is NDC for electrons in radio frequency (rf) fields [52].

On the other hand, there is a whole range of phenomena that can be more easily understood from observations of spatial profiles having in mind spatially resolved local properties, such as the local mean energy (of a sub-swarm) or velocity. For example negative absolute mobility [45, 53] requires a spatial sampling of swarm properties before it could be given a detailed physical explanation [54]. Non-conservative effects often fall into the second category so in this section we look at spatially resolved properties of a positron swarm. If we release a group of charged particles at some point inside a gas very soon the spatial profile will be Gaussian. Due to diffusion it will spread in time, and if there is an external field, it will drift along the direction of the field. Observation of the spatial profile is very informative if considered in conjunction with

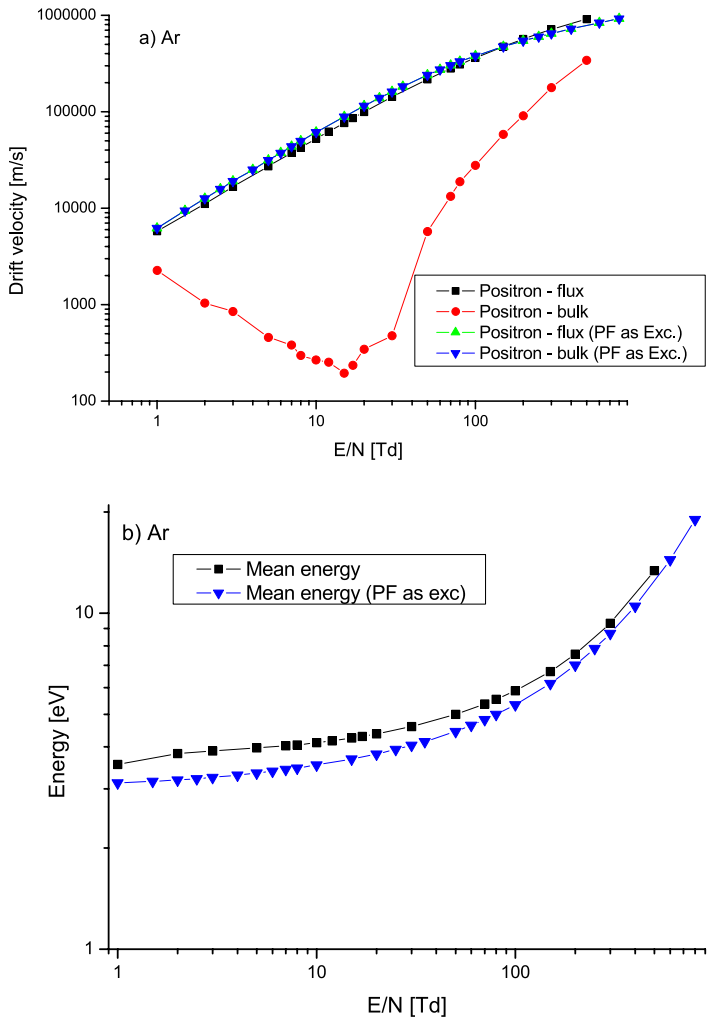

Figure 6. Drift velocities (a) and mean energies (b) for positrons in argon when Ps formation is assumed to be an inelastic process. The NDC effect disappears in the bulk drift velocity and there is only a small difference as compared to the flux drift velocity.

axial profiles of mean energy, mean velocity and rates of different processes. Faster particles moving in the direction of the field will forge ahead leaving slower particles, those with the uphill battle against the field, in their wake. For that reason ionization occurs mostly at the front of the Gaussian, and, for the same reason, effects such as anisotropic diffusion and anomalous diffusion occur [47].

Sampling of an expanding ensemble is difficult as it may be performed only in a single point in space and time. We would prefer to continue sampling over a longer period. The first approach is very wasteful as one needs to bring charged particles into the hydrodynamic regime, i.e. into the regime where all the initial conditions are 'forgotten' by the ensemble. As a result, we would have to follow a lot of particles over a long time only to abandon them as soon as they become useful and contribute to the sampling. Thus, we have developed a procedure that defines the coordinate system not in real space but in real space normalized to six standard deviations. Thus, in spite of broadening of the Gaussian we may easily position each particle to its place

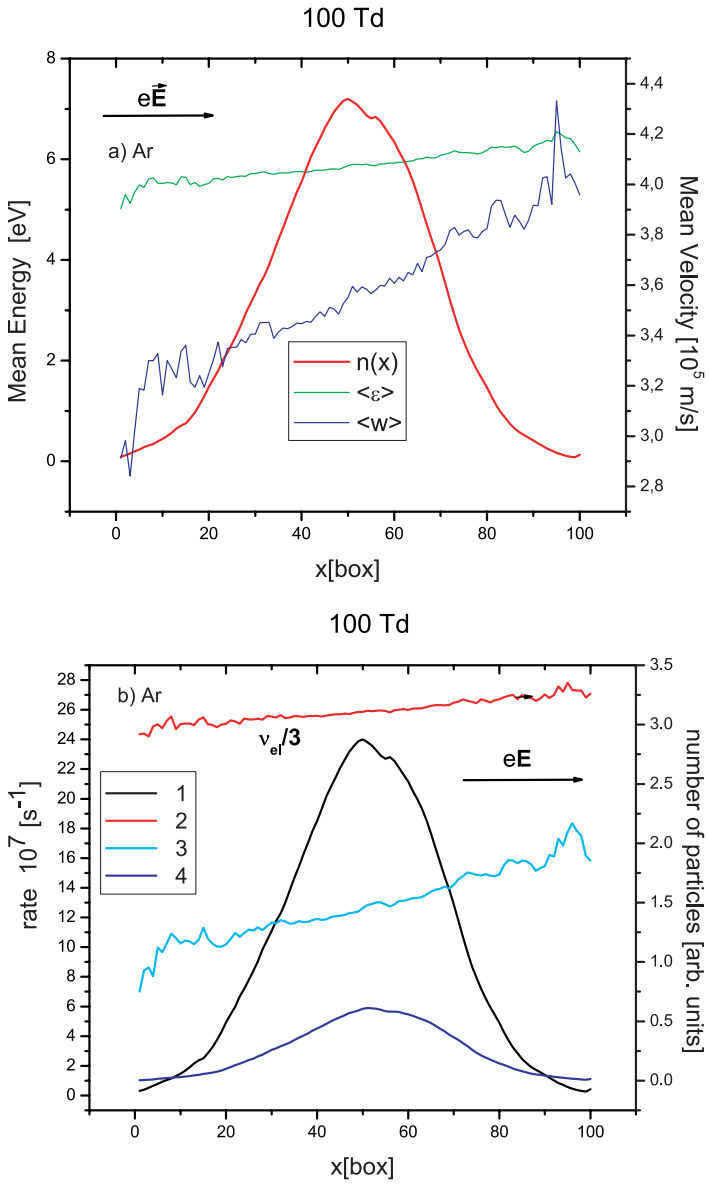

Figure 7. Spatial profile of the positron swarm at 100 Td. (a) Spatial profile of the swarm, axial profile of mean energy and drift velocity. (b) Spatial profile of the swarm (1), elastic rate coefficient (divided by 3) (2), rate of Ps formation (3) number of Ps formations (4).

along the normalized Gaussian profile regardless of the moment when sampling was performed. That way we may use particles that have reached equilibrium (with the field not thermodynamic equilibrium) over and over again, wasting our computing effort on thermalization only once, at the beginning.

First, we show the spatial profile of the swarm at 100 Td (figure 7). While it is not a perfect Gaussian it is still basically symmetric. At the same time all spatial profiles of the properties show weak dependence on axial position, i.e. mean energy, Ps formation rate and other processes occur more frequently at the front of the distribution but the dependence is almost linear. The

slopes are quite high and the spatial differentiation of particles equals or exceeds that usually found for electrons and, following the quickly rising mean energy, the rate of Ps formation rises toward the front of the swarm. At the same time, due to high mean energies, the spatial profile of Ps formation events is symmetric and to a large degree follows the profile of the swarm.

If we go to 5 Td, to the center of the NDC effect, we see a significantly different profile. It is no longer a symmetric Gaussian as it always is for electrons. The front end seems to be cut off. More important are the differences in the spatial profiles of mean energy, velocity and rates. Mean energy seems to be almost constant in the back of the swarm and suddenly, and with a much steeper slope, it starts increasing towards the front of the swarm from 1 to 10 eV. Also the average velocity increases in a nonlinear fashion.

The elastic rate has a complex profile that is associated with the overlap of the mean energy and the corresponding cross section. Positronium formation is relatively small except at the front where it peaks. Inelastic processes peak even further away at the very front of the swarm. Both rate coefficients and total rates peak at the front but their magnitude is such that they can affect the shape of the swarm. As a result the shape is asymmetric because of the spatial profile of Ps formation. If not for Ps formation, the Gaussian would have been almost symmetric with a peak occurring much further to the right, close to where the front of the swarm is now. However, the high energy particles are 'eaten' away due to annihilation with matter. With the result being, the center is shifted to the left and the profile is highly skewed.

In summary, positrons that are accelerated by the field reach energies where Ps formation reigns and then they will most likely disappear. In the energy region, where Ps formation is the dominant process (with the exception of elastic scattering) positrons disappear before they can gain sufficient energy to be accelerated in the direction of the field. This is exactly why the measured drift velocity drops by two orders of magnitude and the longitudinal diffusion coefficient becomes almost zero in this region.

At the same time, the positrons moving in the other direction do not have enough energy for Ps formation and thus their distribution is not changed. The resulting flux drift velocity (averaged over the energy distribution function and all positions) and transverse diffusion coefficients are thus considerably higher (i.e. they have 'normal' values for similar mean energies of electrons). The mean energies, are those that are expected for these values of E/N.

The extreme skewing of the spatial profile enhances the effect on the bulk velocity as compared to the predictions of Vrhovac and Petrovic [6] given by equation (6). This is due to the fact that their theory was not able to include such spatial profile variations. So their theory is correct in principle and it provides the physical foundation for the bulk drift velocity NDC but quantitative comparisons should be done with results of simulations that may accommodate arbitrary spatial profiles.

Model calculation presented in figure 6 is a very direct proof that our explanation of NDC for the bulk positron drift velocity is correct. The difference between figures 7 and 8 shows that the spatially localized, non-conservative nature of Ps formation in positron transport leads to effects that are consistent with this specific form of NDC. The spatial localization of Ps formation in the profile of the swarm may not be sufficient for the bulk drift velocity NDC to develop, as the effect may depend on the degree of spatial deformation of the swarm. However, it is a proof that such an effect is necessary, as without such an effect, the bulk drift velocity NDC would be impossible.

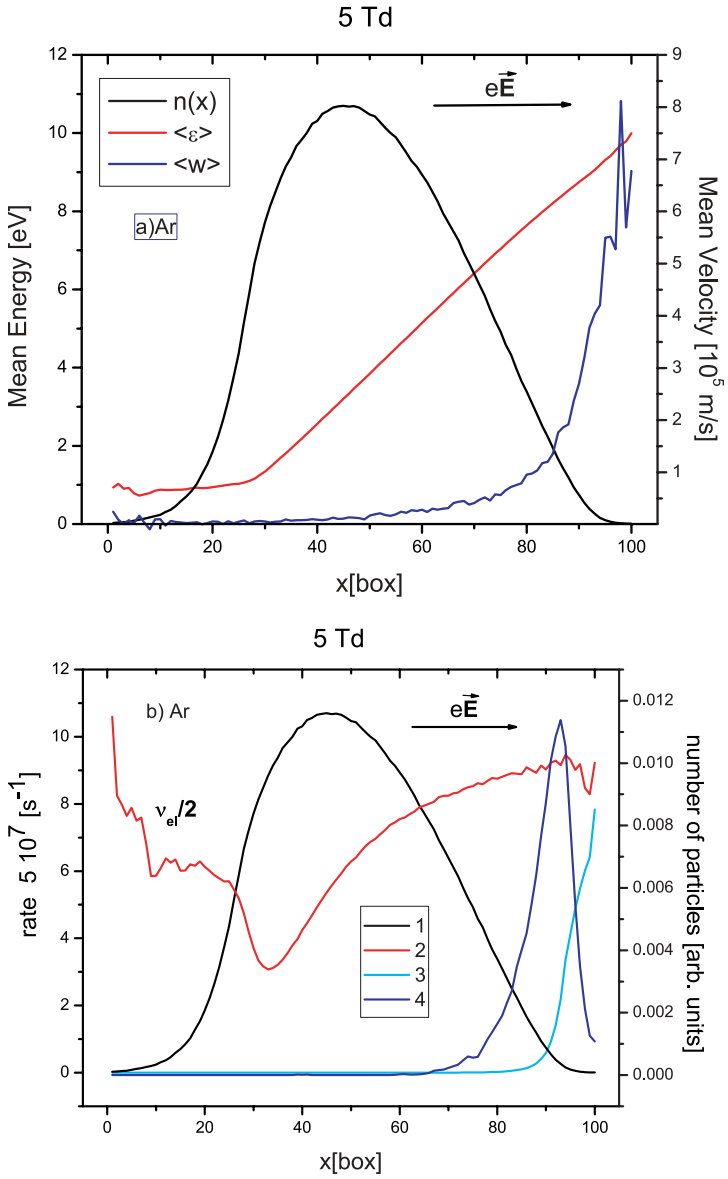

Figure 8. Spatial profile of the positron swarm in argon at 5 Td. (a) Spatial profile of the swarm, axial profile of mean energy and drift velocity. (b) Spatial profile of the swarm (1), elastic rate coefficient (divided by 2) (2), rate of Ps formation (3), number of Ps formations (4).

5. Conclusion

In this paper, we have compiled a reasonably accurate and complete set of cross sections for low energy positrons in argon. The dominant feature is the Ps formation cross section which is greater than the elastic scattering cross section in a range of energies and also which dominates positron transport for energies below the threshold for electronic excitation. Due to this large cross section for Ps formation, non-conservative processes dominate the transport of positrons. While the mean energy and the relevant characteristic energies have values and shapes similar

to those for electrons in the same gas, the bulk drift velocities show a major departure from those seen for electrons. While the flux drift velocity is of the expected magnitude and has a steady increase with E/N, thus making NDC unlikely, the bulk drift velocity has a pronounced minimum associated with NDC. A similar effect (i.e. a minimum and a value close to zero) is observed for longitudinal diffusion.

It was predicted in [6] that the bulk drift velocity may show NDC (for electrons only if conditions are met or almost met for the flux drift velocity) due to non-conservative processes. This theory gives good qualitative guidance as to what may be expected. On the other hand, the basic phenomenology has been confirmed by making test simulations with the replacement of the Ps formation by an inelastic process of the same magnitude and energy dependence. For this model there is no effect and thereby it is concluded that the observed NDC is induced by the non-conservative nature of Ps formation. This is supported by observation of the spatial profile of positron swarms, where in the region of NDC there is a large degree of skewness [55] of the profile.

The behavior of the drift velocity may have been observed experimentally in hydrogen as the calculated flux drift velocity [56] does not show the NDC, while experimental observations [29] show a pronounced NDC. Our observations may also be relevant for earlier modeling of thermal positron swarms below the threshold for excitation [13].

The present data may also be used to estimate the thermalization times or ranges in a possible design of future swarm-like experiments. For example, momentum relaxation may be estimated as D/w (as verified by Monte Carlo simulations of Braglia and Lowke [57]). In a similar fashion thermalization times may be estimated from the transport data [58]. However, it seems much more appropriate not to describe the 'non-hydrodynamic' development of swarms by 'hydrodynamic' transport parameters, as each act of Monte Carlo simulation actually passes through the stage of relaxation from the initial conditions. So it is only required to select a realistic set of initial conditions and perform the simulation, with a possible extension of the cross section range if required. Nevertheless, even rough estimates that may be based on the presently derived data may be applied in designing experiments. In addition, thermalization studies of the transport in rf fields may be worthwhile.

It has been only 75 years since the experimental discovery of positrons [59]. During that period positrons have become invaluable in numerous applications that involve maintaining and controlling their properties (energy in particular) within the constituents of matter [1]. As the ability to control and manipulate positrons improves, positrons are finding more practical applications in the fields of biology, medicine and material science. Most often these applications involve thermalized positron 'swarms'. Therefore, besides being of fundamental interest, knowledge of these transport coefficients is expected to be of practical interest to those interested in developing or improving these technologies. In particular, one of our immediate goals involves studies of positron transport in water, the dominant constituent of living tissue. Additionally, we hope to progress modern transport phenomenology, theory and simulations for positrons to the same level as that for electrons [44, 47] in a hope that experimental studies will soon follow.

Acknowledgments

This work has been funded by the MNTRS project 141025 and by FP6 project 026328 IPB-CNP. We are grateful to our colleagues M Charlton, S Dujko, R White, J P Sullivan and

R P McEachran for useful information and their suggestions. In particular, we are grateful to A Banković for helping us with preparation of some of the final sets of data. SJB and RER are grateful to the Australian Research Council for support under the Centres of Excellence Program and to the Australian Government Department of Innovation, Industry, Science and Research for support under the International Science Linkages Programme.

References

[1] Charlton M and Humberston J 2000 *Positron Physics* (New York: Cambridge University Press)
[2] Sullivan J P, Gilbert S J and Surko C M 2001 *Phys. Rev. Lett.* **86** 1494
[3] Sullivan J P, Gilbert S J, Marler J P, Greaves R G, Buckman S J and Surko C M 2002 *Phys. Rev.* A **66** 042708
[4] Marler J P, Sullivan J P and Surko C M 2005 *Phys. Rev.* A **71** 022701
[5] Laricchia G, Reeth P V, Szłuińska M and Moxom J 2002 *J. Phys. B: At. Mol. Opt. Phys.* **35** 2525
[6] Vrhovac S B and Petrović Z Lj 1996 *Phys. Rev.* E **53** 4012
[7] Muehllehner G and Karp J S 2006 *Phys. Med. Biol.* **51** R117
[8] Cassidy D B, Yokoyama K T, Deng S H M, Griscom D L, Tom H W, Varma C M and Mills A P Jr 2007 *Phys. Rev.* B **75** 085415
[9] Sato K, Yoshiie T, Ishizaki T and Xu Q 2007 *Phys. Rev.* B **75** 094109
[10] Al-Qaradawi I, Charlton M, Borozan I and Whitehead R 2000 *J. Phys. B: At. Mol. Opt. Phys.* **33** 2725
[11] Davies S A, Charlton M and Griffith T C 1989 *J. Phys. B: At. Mol. Opt. Phys.* **22** 327
[12] Charlton M 1985 *Rep. Prog. Phys.* **48** 737
[13] Farazdal A and Epstein I R 1978 *Phys. Rev.* A **1** 577
[14] Gilbert S J, Greaves R G and Surko C M 1999 *Phys. Rev. Lett.* **82** 5032
[15] Cassidy D B, Deng S H M, Greaves R G and Mills Jr A P 2006 *Rev. Sci. Instrum.* **77** 073106
[16] Nikitović Ž D, Strinić A I, Stojanović V D, Malović G N and Petrović Z Lj 2007 *Radiat. Phys. Chem.* **76** 556
[17] Li B, Robson R E and White R D 2006 *Phys. Rev.* E **74** 026405
[18] Robson R E 1986 *J. Chem. Phys.* **85** 4486
[19] Ness K F and Robson R E 1986 *Phys. Rev.* A **34** 2186
[20] Raspopović Z M, Sakadžić S, Bzenić S and Petrović Z Lj 1999 *IEEE Trans. Plasma Sci.* **27** 1241
[21] Dujko S, White R D, Ness K F, Petrović Z Lj and Robson R E 2006 *J. Phys. D: Appl. Phys.* **39** 4788
[22] Petrović Z Lj, Crompton R W and Haddad G N 1984 *Aust. J. Phys.* **37** 23
[23] Robson R E 1984 *Aust. J. Phys.* **37** 35
[24] Blake D and Robson R E 2001 *J. Phys. Soc. Japan* **70** 3556
[25] Raspopović Z M, Sakadžić S, Petrović Z Lj and Makabe T 2000 *J. Phys. D: Appl. Phys.* **33** 1298
[26] Dujko S, Raspopović Z M, Petrović Z Lj and Makabe T 2003 *IEEE Trans. Plasma Sci.* **31** 711
[27] Maeda K, Makabe T, Nakano N, Bzenić S and Petrović Z Lj 1997 *Phys. Rev.* E **55** 5901
[28] Dyatko N A 2007 *J. Phys.: Conf. Ser.* **71** 012005
[29] Bose N, Paul D A L and Tsai J S 1981 *J. Phys. B: At. Mol. Phys.* **14** L227
[30] Charlton M 1985 *J. Phys. B: At. Mol. Phys.* **18** L667
[31] Iwata K, Gribakin G, Greaves R G and Surko C M 2000 *Phys. Rev.* A **A61** 022719
[32] Petrović Z Lj, Šuvakov M, Nikitović Ž, Dujko S, Šašsić O, Jovanović J, Malović G and Stojanović V 2007 *Plasma Sources Sci. Technol.* **16** S1
[33] Surko C M, Gribakin G F and Buckman S J 2005 *J. Phys. B: At. Mol. Opt. Phys.* **38** R57
[34] Karwasz G P, Pliszka D and Brusa R S 2006 *Nucl. Instrum. Methods* B **247** 68
[35] McEachran R P 2006 Private communication
[36] Gianturco F A, Jain A and Rodriguez-Ruiz J A 1993 *Phys. Rev.* A **48** 4321
[37] Sullivan J P, Marler J P, Gilbert S J, Buckman S J and Surko C M 2001 *Phys. Rev. Lett.* **87** 073201
[38] Parcell L A, McEachran R P and Stauffer A 2000 *Nucl. Instrum. Methods* B **171** 113
[39] Phelps A V and Tachibana K 1985 Private communication

[40] Barnes L D 2005 *PhD Thesis* University of California, San Diego
[41] Šuvakov M, Ristivojević Z, Petrović Z L, Dujko S, Raspopović Z M, Dyatko N A and Napartovich A P 2005 *IEEE Trans. Plasma Sci.* **33** 532
[42] Petrović Z Lj, Raspopović Z M, Dujko S and Makabe T 2002 *Appl. Surf. Sci.* **192** 1
[43] Robson R E, White R D and Petrović Z Lj 2005 *Rev. Mod. Phys.* **77** 1303
[44] Robson R E 2006 *Introductory Transport Theory for Charged Particles in Gases* (Singapore: World Scientific)
[45] Robson R E, Petrović Z Lj, Raspopović Z M and Loffhagen D 2003 *J. Chem. Phys.* **119** 11249
[46] Robson R E 1991 *Aust. J. Phys.* **50** 577
[47] Makabe T and Petrović Z Lj 2006 *Plasma Electronics: Applications in Microelectronic Device Fabrication* (New York: CRC Press)
[48] Phelps A V ftp://jila.colorado.edu/collisiondata /electronneutral/electron.txt
[49] Sakai Y, Tagashira H and Sakamoto S 1972 *J. Phys. B: At. Mol. Phys.* **5** 1010
[50] Sakai Y, Tagashira H and Sakamoto S 1977 *J. Phys. D: Appl. Phys.* **10** 1035
[51] Kumar K, Skullerud H R and Robson R E 1980 *Aust. J. Phys.* **33** 343
[52] Bzenić S, Petrović Z L, Raspopović Z M and Makabe T 1999 *Japan J. Appl. Phys.* **38** 6077
[53] Dyatko N A, Napartovich A P, Sakadžić S, Petrović Z Lj and Raspopović Z 2000 *J. Phys. D: Appl. Phys.* **33** 375
[54] Petrović Z Lj 1985 *PhD Thesis* Australian National University, Canberra
[55] Vrhovac S B, Petrović Z Lj, Viehland L A and Santhanam T S 1999 *J. Chem. Phys.* **110** 2423
[56] Banković A, Marler J P, Petrović Z Lj and Malović G 2008 unpublished
[57] Braglia G L and Lowke J J 1979 *J. Phys. D: Appl. Phys.* **12** 1831
[58] Christophorou L G, Gant K S and Baird J K 1975 *Chem. Phys. Lett.* **30** 104
[59] Anderson C 1933 *Phys. Rev.* **43** 491